8-1-2006

The B supergiant components of the double-lined binary HD 1383

T. S. Boyajian
Georgia State University

D. R. Gies
Georgia State University

M. E. Helsel
Georgia State University

A. B. Kaye
Georgia State University

M. V. Mcswain
Georgia State University

See next page for additional authors

Recommended Citation

Boyajian, T., Gies, D., Helsel, M., Kaye, A., Mcswain, M., Riddle, R., & Wingert, D. (2006). The B supergiant components of the double-lined binary HD 1383. *Astrophysical Journal, 646* (2 I), 1209-1214. https://doi.org/10.1086/504973

The B-Supergiant Components of the Double-Lined Binary HD 1383

T. S. Boyajian, D. R. Gies[1], M. E. Helsel[2], A. B. Kaye[1],
M. V. McSwain[1,3,4], R. L. Riddle[1,5], D. W. Wingert[1]

Center for High Angular Resolution Astronomy and
Department of Physics and Astronomy,
Georgia State University, P. O. Box 4106, Atlanta, GA 30302-4106;
tabetha@chara.gsu.edu, gies@chara.gsu.edu, marian.helsel@furman.edu,
anthony.kaye@itt.com, mcswain@astro.yale.edu, riddle@astro.caltech.edu,
wingert@chara.gsu.edu

ABSTRACT

We present new results from a study of high quality, red spectra of the massive binary star system HD 1383 (B0.5 Ib + B0.5 Ib). We determined radial velocities and revised orbital elements ($P = 20.28184 \pm 0.0002$ d) and made Doppler tomographic reconstructions of the component spectra. A comparison of these with model spectra from non-LTE, line blanketed atmospheres indicates that both stars have almost identical masses ($M_2/M_1 = 1.020 \pm 0.014$), temperatures ($T_{\rm eff} = 28000 \pm 1000$ K), gravities ($\log g = 3.25 \pm 0.25$), and projected rotational velocities ($V \sin i \lesssim 30$ km s^{-1}). We investigate a number of constraints on the radii and masses of the stars based upon the absence of eclipses, surface gravity, stellar wind terminal velocity, and probable location in the Perseus spiral arm of the Galaxy, and these indicate a range in probable radius and mass of $R/R_\odot = 14 - 20$ and $M/M_\odot = 16 - 35$, respectively. These values are consistent

[1]Visiting Astronomer, Kitt Peak National Observatory, National Optical Astronomy Observatory, operated by the Association of Universities for Research in Astronomy, Inc., under contract with the National Science Foundation.

[2]Current Address: Department of Chemistry, Furman University, 3300 Poinsett Highway, Greenville, SC 29613

[3]Current Address: Astronomy Department, Yale University, New Haven, CT 06520-8101

[4]NSF Astronomy and Astrophysics Postdoctoral Fellow

[5]Current Address: Department of Astronomy, California Institute of Technology, 305 S. Hill Ave., MC 102-8, Pasadena, CA 91125

with model evolutionary masses for single stars of this temperature and gravity. Both stars are much smaller than their respective Roche radii, so the system is probably in a pre-contact stage of evolution. A fit of the system's spectral energy distribution yields a reddening of $E(B-V) = 0.55 \pm 0.05$ and a ratio of total-to-selective extinction of $R = 2.97 \pm 0.15$. We find no evidence of Hα emission from colliding stellar winds, which is probably the consequence of the low gas densities in the colliding winds zone.

Subject headings: binaries: spectroscopic — stars: early-type — stars: evolution — stars: individual (HD 1383) — supergiants — stars: winds, outflows

1. Introduction

The evolutionary paths of massive binaries depend critically on processes related to mass transfer and mass loss at the time when the initially more massive star begins to fill its Roche volume (Langer et al. 2004; Petrovic, Langer, & van der Hucht 2005). On the one hand, mass from the donor star may end up entirely in a rejuvenated mass gainer, but on the other hand a high mass transfer rate may cause the gainer to swell and bring the system into a common envelope phase, in which most of the donor's mass is lost from the system entirely. Evidence of both outcomes is found among post-Roche lobe overflow systems (Langer et al. 2004; Petrovic et al. 2005). We can better constrain the problem of the probable results of the interaction by studying binaries in an advanced evolutionary state just prior to Roche-filling. Those binaries of nearly identical masses are particularly interesting because we can usually observe the spectra of both components.

Close pairs of nearly identical, evolved massive stars are quite rare. The HD 1383 system is the only such system found in *Ninth Catalogue of Spectroscopic Binary Orbits* (Pourbaix et al. 2004) (with identical components of types B0.5 Ib + B0.5 Ib; Hill & Fisher 1986). Another similar massive stellar system, HD 152248, was previously classified as a O7 I + O7 I (Penny, Gies, & Bagnuolo 1999), although a more thorough analysis by Sana et al. (2001) revised the classifications to O7.5 III + O7 III, deviating from the exact match of types found in HD 1383. The HD 152248 system is eclipsing and the mass determinations made by Penny et al. (1999) and Sana et al. (2001) indicate that both stars are undermassive (by factors of 2 and 1.4, respectively, in the two studies) relative to the predicted evolutionary masses for single stars. Here we focus our attention on HD 1383 (BD+60°25, HIP 1466). The system was identified as a double-lined binary early on (Sanford & Merrill 1938; Slettebak 1956), but the first orbital elements were determined later by Hill & Fisher (1986) who found that the system consists of two nearly identical stars with an orbital period of 20.3 d. Morgan,

Code, & Whitford (1955) originally adopted the system as a spectral standard for the B1 II type, but Hill & Fisher (1986) revised the types slightly based upon detailed measurements of line equivalent widths of both components. The system is located in the sky in the vicinity of the Cas OB4 association (Humphreys 1978), which is located in the Perseus arm of the Galaxy. The star has played an important role in studies of the interstellar medium in this direction (see Cartledge et al. 2004). Various distances have been estimated based upon the assumption that HD 1383 is a single, B1 II star. Wakker et al. (1998) found a distance of 1.7 kpc, which agrees well with Humphreys (1978) value of 1.68 kpc. Humphreys (1978) noted that HD 1383 might not be a member of the Cas OB4 association, because the latter has a greater distance of 2.88 kpc. However, the fact that HD 1383 is a binary consisting of two stars with approximately equal brightness implies that it farther away from us than these previous estimates indicate and that it is closer to Cas OB4 (Hill & Fisher 1986 offer a distance 3.0 kpc for HD 1383).

Here we present a study of a set of red spectra of HD 1383 that we obtained (§2) to re-analyze the orbital elements (§3) and to search for evidence of Hα emission related to colliding winds (Thaller 1997; Sana et al. 2001). We discuss the physical parameters of the stars from an analysis of their individual spectra obtained from a Doppler tomography reconstruction (§4). We then present a number of constraints on the radii and masses of the stars (§5) that lead us to conclude that both stars have radii smaller than their Roche radii and luminosities that are too small to power strong winds (explaining the lack of Hα emission from colliding winds).

2. Observations and Radial Velocities

The optical spectra of HD 1383 were obtained with the Kitt Peak National Observatory 0.9 m coudé feed telescope during four observing runs between 1999 August and 1999 December. Most of these spectra were obtained with the short collimator and grating RC181 (316 grooves mm^{-1} with a blaze wavelength of 7500 Å; made in first order with a GG495 filter to block higher orders), which yielded an average resolving power of $R = \lambda/\delta\lambda = 4000$ (see Gies et al. 2002a for details of each observing run). The last four spectra were made with grating B (632 grooves mm^{-1} with a blaze wavelength of 6000 Å in second order) and these have a much higher resolving power, $R = \lambda/\delta\lambda = 21300$. Exposure times varied from 20 to 30 minutes. These spectra all cover a common spectral range between 6456 Å and 6728 Å, and they generally have a S/N $\approx$ 340 pixel^{-1} in the continuum. The spectra were

extracted and calibrated using standard routines in *IRAF*[6], and then each continuum rectified spectrum was transformed onto a uniform heliocentric wavelength grid for analysis. Atmospheric telluric lines were removed by division of modified versions of spectra of the rapidly rotating A-star ζ Aql that we also observed (Gies et al. 2002a).

We measured radial velocities for HD 1383 using a template fitting method (Gies et al. 2002b). The red spectrum of HD 1383 has few lines in the region observed. Hα was not used in the radial velocity analysis because it is too broad and the components are generally blended. The lines of C II $\lambda\lambda 6578, 6582$ and O II $\lambda\lambda 6641, 6721$ are very weak and difficult to measure in individual spectra. Thus, we focused on the remaining, problem-free line of He I $\lambda 6678$ for this radial velocity study. The individual component lines are quite narrow, symmetric, and comparable in shape to the instrumental broadening function, so we chose to represent each component's profile as a Gaussian function. We selected appropriate shape parameters by fitting Gaussians to the best separated profiles of He I $\lambda 6678$, and we used the average values of the parameters to create separate Gaussian absorption line profiles to represent both the primary and secondary stars. We also obtained preliminary orbital velocity curves based upon the Gaussian fits of the well separated spectra, and these were used to estimate the approximate velocities for all the times of observation. We then determined radial velocities for both components in all of our spectra by a non-linear, least-squares fit of the composite profiles, and our results are collected in Table 1, which lists the heliocentric Julian date of mid-exposure, orbital phase from the solution for the primary component, and the observed velocity plus the residual from the fit (observed minus calculated) for both components.

3. Orbital Elements of HD 1383

Hill & Fisher (1986) found that HD 1383 is a double-lined spectroscopic binary with a period of 20.2819 days. We combined our radial velocities (Table 1) with the compilation of radial velocity measurements from Hill & Fisher (1986) for a total 101 and 77 radial velocity measurements (spanning 75 y) of the primary and secondary components, respectively. Using a 'dirty' discrete Fourier transform and CLEAN deconvolution algorithm (Roberts, Lehár, & Dreher 1987), we constructed power spectra for both the primary and secondary using the time series of radial velocity measurements for each. The strongest signal in the power

[6]IRAF is distributed by the National Optical Astronomy Observatory, which is operated by the Association of Universities for Research in Astronomy, Inc., under cooperative agreement with the National Science Foundation.

spectra occurs at $P = 20.3$ days, which we then used as a starting value for the following orbital solutions.

We used the non-linear, least-squares fitting program from Morbey & Brosterhus (1974) to determine orbital elements. We found that our derived velocities were swapped between the primary and secondary for two observations when the components were thoroughly blended, and we assigned zero weight to these measurements in our orbital fit. First, we determined the period of the primary and secondary independently using all the data available, and then we determined a mean value of $P = 20.28184 \pm 0.00020$ d, which we fixed for both stars in the subsequent orbital solutions for HD 1383. Then only the new radial velocity data presented in this paper were used to calculate independent orbital elements for the primary and secondary stars. The separate results for the primary and secondary are presented in Table 2 together with the original results from Hill & Fisher (1986), and the radial velocity curves and observations are plotted in Figure 1. We find that the orbital elements for the primary and secondary are mainly consistent with each other and with the original determinations by Hill & Fisher (1986) with two interesting exceptions. First, the star identified as the "primary" by Hill & Fisher (1986) turns out to be the lower mass object in our solution because of a slight revision in the semiamplitudes. Rather than introducing more confusion about the stars' identities, we will retain the labels of primary and secondary given by Hill & Fisher (1986). Second, we find that the eccentricity derived for the primary is approximately 3σ different from that obtained for the secondary. Furthermore, the longitude of periastron values are suspiciously close to 0° and 180°, which suggests that the velocity curves may be distorted by subtle emission effects from circumstellar gas (the possible origin of the non-uniform distribution of longitude of periastron among massive binaries known as the Barr Effect; Batten & Ovenden 1968; Fracastoro 1979; Howarth 1993). Given these difficulties, we decided not to force a joint solution with a common geometry and systemic velocity.

4. Tomographic Reconstruction and Stellar Parameters

Once the orbital solution was found for HD 1383, we used a tomographic reconstruction technique (Bagnuolo et al. 1994) to separate the two individual spectra of the system. The method of tomographic reconstruction uses all the combined spectra and their associated radial velocities to determine the appearance of each star's spectrum. The monochromatic flux ratio of the primary to the secondary was assumed to be 1.0 (Hill & Fisher 1986). The ISM lines were removed from each spectrum prior to reconstruction to avoid spurious reconstructed features in their vicinity. Figure 2 shows a plot of the reconstructed spectra

with identifications of the principal lines. The two spectra are remarkably similar in the red spectral region.

We made estimates of the effective temperatures, gravities, and projected rotational velocities through a comparison with model spectra from the codes *TLUSTY* and *SYNSPEC* (Hubeny 1988; Hubeny & Lanz 1995; Hubeny, Heap, & Lanz 1998). Lanz & Hubeny (2003) presented a grid of model spectra for O-type stars that use line blanketed, non-local thermodynamic equilibrium, plane-parallel, hydrostatic atmospheres, and fortunately, these models extend to cool enough temperatures (27500 K) to be applicable to the the stars in HD 1383. These models adopt a fixed microturbulent velocity of 10 km s^{-1}, a value which is appropriate for B-supergiants (Gies & Lambert 1992). These models were also used by Dufton et al. (2005) in their spectral analysis of B-supergiants in the SMC.

The projected rotational velocity, $V \sin i$, for each star was measured by comparing the observed FWHM of an absorption line with that for model profiles for a range in assumed $V \sin i$. The rotationally broadened profiles were calculated by a simple convolution of the zero-rotation model profiles with a rotational broadening function (Gray 1992) using a linear limb darkening coefficient $\epsilon = 0.220$ (from the tabulated value for $T_{\rm eff} = 30000$ K, $\log g = 3.0$, and $\lambda = 6975$Å from Wade & Rucinski 1985). The derived projected rotational velocities based upon the He I λ6678 profile are $V \sin i = 76 \pm 6$ and 72 ± 6 km s^{-1} for the primary and secondary, respectively, in good agreement with the estimate of 75 ± 5 km s^{-1} for both stars from measurements of blue spectral lines by Hill & Fisher (1986). However, the weaker C II $\lambda\lambda 6578, 6582$ lines are distinctly narrower and their mean projected rotational velocities are $V \sin i = 32 \pm 18$ and 26 ± 18 km s^{-1} for the primary and secondary, respectively (almost unresolved at our spectral resolution). Ryans et al. (2002) argue that the line broadening of B-supergiants is probably dominated by macroturbulence, so that the measured broadening only provides an upper limit on the actual rotational velocity. They also find a trend for stronger lines (like He I λ6678) to display greater broadening than weaker lines (like C II $\lambda\lambda 6578, 6582$), perhaps due to an increase in turbulent broadening with height in the atmosphere. Thus, the true projected rotational velocities of the components of HD 1383 are probably less than ≈ 30 km s^{-1}.

We then compared rotationally broadened versions of the model solar abundance spectra from Lanz & Hubeny (2003) directly with the reconstructed spectra to estimate temperatures and gravities. The best matches were found with $T_{\rm eff} = 28000 \pm 1000$ K and $\log g = 3.25 \pm 0.25$ for both stars, and the model spectra for these parameters are shown in Figure 2 as dotted lines. This spectral region contains a number of features that are particularly sensitive to temperature and gravity. For example, at hotter temperatures the C II, O II, and He I lines weaken while new lines of Si IV $\lambda\lambda 6667, 6701$ and He II λ6683 appear that are clearly absent

in the reconstructed spectra of HD 1383. On the other hand, at cooler temperatures the C II doublet increases greatly in strength and the N II λ6610 line first appears (again absent in the reconstructed spectra). The wings of the Hα line provide a diagnostic of the gravity (wider due to greater linear Stark broadening in higher gravity models). We caution that the core of Hα appears to be filled in with residual emission from the stellar wind, and the TLUSTY models we used are based upon static atmospheres that do not account for wind outflow. However, we expect that the wind effects will be mainly confined to the higher opacity line core in relatively weak-wind stars like those in HD 1383 and that the gravity derived from the pressure-broadened line wings will be close to (or slightly less) than the actual gravity (see the discussion about the Hγ line wings in Puls et al. 1996). The observed C II lines appear to be somewhat weaker than predicted in the best matching model spectrum, which may reflect an underabundance of C caused by mixing of CNO-processed gas into the atmosphere. McErlean, Lennon, & Dufton (1999) also observed this effect in other B-supergiants. They give model fitting results for two galactic B0.5 Ib stars, HD 192422 and HD 213087, and their derived temperatures and gravities are in reasonable agreement with our adopted values for HD 1383. We found that the generally good match between the model and observed spectra indicates that the monochromatic flux ratio is 1.0 ± 0.1.

5. Discussion

We can use our results to place some general constraints on the evolutionary status of the binary system. These various limits are summarized in a radius–mass diagram for the secondary star shown in Figure 3 (the corresponding diagram for the primary would appear almost the same). The system is not a known eclipsing binary, and we confirmed the lack of eclipses (or any other orbital phase-related variations) by plotting the available photometry from *Hipparcos* (Perryman 1997) as a function of orbital phase. If we assume that the stars have the same radius R (as indicated by their temperatures and the observed flux ratio), then the upper limit on the orbital inclination i set by the lack of eclipses is found from

$$\tan i = \frac{a \sin i}{2R} \frac{1 - e^2}{1 + e \cos \nu}. \quad (1)$$

We considered both conjunctions, $\nu = 90^\circ - \omega$ and $270^\circ - \omega_2$, with the derived eccentricities for the primary and secondary to find the minimum inclination for a given radius and hence a lower limit on the mass of the secondary from $M_2 \sin^3 i$ (Table 2), and the resulting radius–mass relationships are plotted as dashed lines in Figure 3. The acceptable solution space is restricted to the region above these lines (at lower i). The next constraint comes from the gravity determination found by fitting the Hα line wings, and the solid lines in Figure 3

show the relations for $\log g = 3.25 \pm 0.25$. If weak stellar wind emission is biasing this measurement, then the actual $\log g$ may be somewhat larger than our estimate.

We can use the stellar wind properties to find additional limitations. Theoretical and observational studies of the winds of massive stars show that the wind terminal velocity v_∞ is generally proportional to the escape velocity $v_{\rm esc}$ among stars of comparable temperature (Prinja, Barlow, & Howarth 1990; Lamers, Snow, & Lindholm 1995; Kudritzki & Puls 2000; Evans et al. 2004; Crowther, Lennon, & Walborn 2006). Prinja et al. (1990) have made the most complete study of this relationship among the B-supergiants, and they find that $v_\infty = (1.96 \pm 0.60) v_{\rm esc}$ for B0-B3 I stars. We measured the terminal velocity to be $v_\infty = 1100 \pm 120$ km s^{-1} according to the short wavelength absorption minimum point in the profile of the C IV λ1550 P Cygni line in a high dispersion spectrum of HD 1383 from the archive of the *International Ultraviolet Explorer Satellite* (made at orbital phase $\phi = 0.21$, near conjunction). This terminal velocity is somewhat lower than the mean for the B0.5 supergiants of 1405 km s^{-1} but it is well within the range of terminal velocities for this group (Prinja et al. 1990). We show the resulting radius–mass functions from the mean and $\pm 1\sigma$ limits of the $v_\infty / v_{\rm esc}$ relation in Figure 3 (*triple dot-dashed line*). Note that the larger values of this ratio found in recent studies (Evans et al. 2004; Crowther et al. 2006) are probably more appropriate for much more luminous stars and would lead to unrealistically large radii in the case of HD 1383.

Finally, we can obtain one more constraint by considering the radius–distance relationship that is established from fits of the reddened stellar flux distribution. We show in Figure 4 the observed spectral energy distribution for HD 1383 based upon low dispersion UV spectroscopy from *IUE*, Johnson U, B, V magnitudes (Haug 1970; Colina, Bohlin, & Castelli 1996), and 2MASS J, H, K infrared magnitudes (Cohen, Wheaton, & Megeath 2003; Cutri et al. 2003). We fit this flux distribution using a model spectrum from Lanz & Hubeny (2003) for two identical stars of $T_{\rm eff} = 28000$ K and $\log g = 3.25$, which we transformed using the Galactic extinction curve from Fitzpatrick (1999). The best fit parameters for the extinction curve are a reddening of $E(B-V) = 0.55 \pm 0.05$ and a ratio of total-to-selective extinction of $R = 2.97 \pm 0.15$. The normalization of the model spectrum yields the limb darkened angular diameter of one star, $\theta_{LD} = 54 \pm 7$ microarcsec, and therefore the stellar radius is related to the distance d (measured in kpc) by

$$R/R_\odot = (5.8 \pm 0.8) d. \tag{2}$$

The binary is too distant to obtain a reliable parallax from *Hipparcos* measurements (Schröder et al. 2004). Our view through the plane of the Galaxy in the direction of HD 1383 ($l = 119\overset{\circ}{.}02$, $b = -0\overset{\circ}{.}89$) traverses first the nearer Perseus arm ($d = 2.4 - 3.5$ kpc) and then the more distant Cygnus arm ($d \gtrsim 3.9$ kpc) (Kimeswenger & Weinberger 1989; Negueruela

& Marco 2003). We suspect that HD 1383 resides in the closer Perseus arm. It is very close in the sky to BD+60°39 (spectral classification of O9 V), which has an identical reddening and which Garmany & Stencel (1992) assign to the Cas OB4 association (at a distance of 2.8 kpc). There is a considerable amount of differential Galactic rotation along this line of sight, and we can estimate at what distance the systemic velocity of the binary matches the expected radial velocity difference between the Sun and the remote local standard of rest. We used the procedure described by Berger & Gies (2001) to find the distance–radial velocity relation along this line of sight, and the binary's systemic velocity places it at a distance of 3.2 kpc (although if we allow a ± 10 km s^{-1} deviation in motion from the local standard of rest, then the acceptable range is between 2.3 and 4.2 kpc). Both lines of evidence are consistent with a location in the Perseus arm, and we have plotted the corresponding stellar radius range as a solid line in the bottom of Figure 3.

The combination of all these constraints indicates that the parameter ranges are probably $R/R_\odot = 14 - 20$ and $M/M_\odot = 16 - 35$. This range is consistent with the masses predicted by single star evolutionary tracks for the temperature and gravity of the components in HD 1383 (illustrated in Figure 3 as a dotted line, from the evolutionary tracks for non-rotating, solar metallicity stars of $T_{\rm eff} = 28000$ K; Schaller et al. 1992). The radii are much smaller than the Roche lobe radii (approximately $44R_\odot$ for masses of $25M_\odot$), so the system is probably still observed in a pre-contact phase in which both stars have evolved like single objects.

We originally selected HD 1383 as a possible target for exhibiting Hα emission from colliding winds (Thaller 1997). However, our spectra show no obvious signs of such Hα emission. We show in Figure 5 the Hα profiles arranged as a function of orbital phase, and the variations appear to be entirely consistent with the motion of the photospheric Hα lines of both components. Sana et al. (2001) found evidence of a weak, broad, and stationary Hα emission feature in their spectra of the similar colliding winds binary HD 152248, and they argue that the emission forms in a planar collision zone between the stars. The lack of Hα colliding winds emission in the spectrum of HD 1383 is probably due to three significant differences between these binary systems. First, the mass loss rates are lower in HD 1383 compared to HD 152248. We can estimate approximately the mass loss rates using the wind momentum relation for hot stars,

$$\log(\dot{M} v_\infty (R/R_\odot)^{1/2}) = \log D_0 + x \log(L/L_\odot) \qquad (3)$$

where D_0 and x are constants and L is the stellar luminosity (Kudritzki & Puls 2000; Vink, de Koter, & Lamers 2000). If we adopt $T_{\rm eff} = 28000$ K, $R/R_\odot = 14 - 20$, and $v_\infty = 1100$ km s^{-1}, then the predicted mass loss rate is $\log \dot{M} = -6.3 \pm 0.4$ (units of $M_\odot$ y^{-1}) according to the model of Vink et al. (2000), which is about six times lower than the mass loss rates

of the stars in HD 152248 (Sana et al. 2004). Second, the binary separation is about twice as large in HD 1383 compared to HD 152248 (Sana et al. 2004), and hence the wind density in the regions near the collision zone will be much lower. Third, the collision zone itself may cool less efficiently and may avoid the formation of high density gas fragments that are predicted to occur according to hydrodyanmical simulations of the winds of HD 152248 (Sana et al. 2004). Stevens, Blondin, & Pollock (1992) show how the gas dynamics of the colliding winds zone depends on the ratio of the cooling timescale to the gas flow timescale, $\chi \approx v_8^4\ d_{12}/\dot{M}_{-7}$, where v_8 is the wind velocity in units of 1000 km s^{-1}, d_{12} is the distance from the star to the contact surface in units of 10^7 km, and $\dot{M}_{-7}$ is the mass loss rate in units of $10^{-7}\ M_\odot$ y^{-1}. This ratio is about 1.1 for HD 1383, indicating that the collision zone remains hot over dimensions comparable to those of the binary system (an adiabatic wind zone), but the ratio is much smaller (0.1) in the case of HD 152248 where efficient cooling (in a radiative colliding wind) leads to the fragmentation of the shock front into knots of cool gas (Sana et al. 2004). Since Hα emission is a recombination process that depends on the square of the gas density and since the colliding wind density will be much lower in HD 1383 compared to HD 152248 for all of the reasons outlined above, the apparent lack of Hα emission in the spectrum of HD 1383 is not surprising.

Our results indicate that HD 1383 is a wide enough system that the components have avoided direct interaction or mass exchange. According to the models of Schaller et al. (1992), this state may last for another 0.5 Myr (for masses of $25M_\odot$). However, after that time both stars will quickly grow in radius and reach contact within the last 10^4 y before they explode as supernovae. Their brief interaction phase then may result in a common envelope stage leading to a shorter period system containing an O-supergiant and neutron star (like the massive X-ray binary system HD 153919/4U1700–37; Ankay et al. 2001) or in a wider binary consisting of a rapidly evolving B-A supergiant transferring mass at a tremendous rate to a collapsed companion surrounded by a super-Eddington accretion disk (like SS 433; Hillwig et al. 2004). Either way, HD 1383 is destined to become an extraordinarily energetic interacting binary for a brief instant in the Galaxy's future.

We thank Daryl Willmarth and the staff of KPNO for their assistance in making these observations possible. We are also grateful to the referee, Dr. Hughes Sana, for his insight and helpful comments on this study. This work was supported by the National Science Foundation under Grant No. AST-0205297. Institutional support has been provided from the GSU College of Arts and Sciences and from the Research Program Enhancement fund of the Board of Regents of the University System of Georgia, administered through the GSU Office of the Vice President for Research.

REFERENCES

Ankay, A., Kaper, L., de Bruijne, J. H. J., Dewi, J., Hoogerwerf, R., & Savonije, G. J. 2001, A&A, 370, 170

Bagnuolo, W. G., Jr., Gies, D. R., Hahula, M. E., Wiemker, R., & Wiggs, M. S. 1994, ApJ, 423, 446

Batten, A. H., & Ovenden, M. W. 1968, PASP, 80, 85

Berger, D. H., & Gies, D. R. 2001, ApJ, 555, 364

Cartledge, S. I. B., Lauroesch, J. T., Meyer, D. M., & Sofia, U. J. 2004, ApJ, 613, 1037

Cohen, M., Wheaton, W. A., & Megeath, S. T. 2003, AJ, 126, 1090

Colina, L., Bohlin, R., & Castelli, F. 1996, HST Instrument Science Report CAL/SCS-008 (Baltimore: STScI)

Crowther, P. A., Lennon, D. J., & Walborn, N. R. 2006, A&A, 446, 279

Cutri, R. M., et al. 2003, The 2MASS All-Sky Catalog of Point Sources (Pasadena: IPAC/Cal. Inst. Tech.)

Dufton, P. L., Ryans, R. S. I., Trundle, C., Lennon, D. J., Hubeny, I., Lanz, T., & Allende Prieto, C. 2005, A&A, 434, 1125

Evans, C. J., Lennon, D. J., Trundle, C., Heap, S. R., & Lindler, D. J. 2004, ApJ, 607, 451

Fitzpatrick, E. L. 1999, PASP, 111, 63

Fracastoro, M. G. 1979, A&A, 78, 112

Garmany, C. D., & Stencel, R. E. 1992, A&AS, 94, 211

Gies, D. R., & Lambert, D. L. 1992, ApJ, 387, 673

Gies, D. R., McSwain, M. V., Riddle, R. L., Wang, Z., Wiita, P. J., & Wingert, D. W. 2002a,ApJ, 566, 1069

Gies, D. R., Penny, L. R., Mayer, P., Drechsel, H., & Lorenz, R. 2002b, ApJ, 574, 957

Gray, D. F. 1992, The Observation and Analysis of Stellar Photospheres (2nd ed.) (Cambridge: Cambridge Univ. Press)

Haug, U. 1970, A&AS, 1, 35

Hill, G., & Fisher, W. A. 1986, Publ. Dominion Astrophys. Obs., 16, 193

Hillwig, T. C., Gies, D. R., Huang, W., McSwain, M. V., Stark, M. A., van der Meer, A., & Kaper, L. 2004, ApJ, 615, 422

Howarth, I. D. 1993, Observatory, 113, 75

Hubeny, I. 1988, Computer Physics Comm., 52, 103

Hubeny, I., Heap, S. R., & Lanz, T. 1998, in Properties of Hot, Luminous Stars (ASP Conf. Ser. 131), ed. I. D. Howarth (San Francisco: ASP), 108

Hubeny, I., & Lanz, T. 1995, ApJ, 439, 875

Humphreys, R. M. 1978, ApJS, 38, 309

Kimeswenger, S., & Weinberger, R. 1989, A&A, 209, 51

Kudritzki, R.-P., & Puls, J. 2000, ARA&A, 38, 613

Lamers, H. J. G. L. M., Snow, T. P., & Lindholm, D. M. 1995, ApJ, 455, 269

Langer, N., Yoon, S.-C., Petrovic, J., & Heger, A. 2004, in Stellar Rotation, Proc. IAU Symp. 215, ed. A. Maeder & P. Eenens (San Francisco: A.S.P.), 535

Lanz, T., & Hubeny, I. 2003, ApJS, 146, 417

McErlean, N. D., Lennon, D. J., & Dufton, P. L. 1999, A&A, 349, 553

Morbey, C., & Brosterhus, E. B. 1974, PASP, 86, 455

Morgan, W. W., Code, A. D., & Whitford, A. E. 1955, ApJS, 2, 41

Negueruela, I., & Marco, A. 2003, A&A, 406, 119

Penny, L. R., Gies, D. R., & Bagnuolo, W. G., Jr. 1999, ApJ, 518, 450

Perryman, M. A. C. 1997, The Hipparcos and Tycho Catalogues, ESA SP-1200 (Noordwijk: ESA/ESTEC)

Petrovic, J., Langer, N., & van der Hucht, K. A. 2005, A&A, 435, 1013

Pourbaix, D., et al. 2004, A&A, 424, 727

Prinja, R. K., Barlow, M. J., & Howarth, I. D. 1990, ApJ, 361, 607

Puls, J., et al. 1996, A&A, 305, 171

Roberts, D. H., Lehár, J., & Dreher J. W. 1987, AJ, 93, 968

Ryans, R. S. I., Dufton, P. L., Rolleston, W. R. J., Lennon, D. J., Keenan, F. P., Smoker, J. V., & Lambert, D. L. 2002, MNRAS, 336, 577

Sana, H., Rauw, G., & Gosset, E. 2001, A&A, 370, 121

Sana, H., Stevens, I. R., Gosset, E., Rauw, G., & Vreux, J.-M. 2004, MNRAS, 350, 809

Sanford, R. F., & Merrill, P. W. 1938, ApJ, 87, 517

Schaller, G., Schaerer, D., Meynet, G., & Maeder, A. 1992, A&AS, 96, 269

Schröder, S. E., Kaper, L., Lamers, H. J. G. L. M., & Brown, A. G. A. 2004, A&A, 428, 149

Slettebak, A. 1956, ApJ, 124, 173

Stevens, I. R., Blondin, J. M., & Pollock, A. M. T. 1992, ApJ, 386, 265

Thaller, M. L. 1997, ApJ, 487, 380

van Steenberg, M. E., & Shull, J. M. 1988, ApJ, 335, 197

Vink, J. S., de Koter, A., & Lamers, H. J. G. L. M. 2000, A&A, 362, 295

Wade, R. A., & Rucinski, S. M. 1985, A&AS, 60, 471

Wakker, B., van Woerden, H., de Boer, K.S., & Kalberla, P. 1998, ApJ, 493, 762

Table 1. HD 1383 Radial Velocity Measurements

HJD (−2,451,000)	Primary Orbital Phase[a]	V_1 (km s^{-1})	$(O-C)_1$ (km s^{-1})	V_2 (km s^{-1})	$(O-C)_2$ (km s^{-1})
419.951[b]	0.253	−19.9	1.9	−65.0	−20.7
420.950.....	0.302	14.0	3.7	−77.4	1.7
421.869.....	0.347	36.3	2.0	−102.3	3.7
421.891.....	0.348	37.1	2.3	−101.0	5.5
423.865.....	0.445	69.0	2.7	−143.6	−2.4
425.851.....	0.543	71.7	2.2	−144.4	−2.5
425.875.....	0.545	70.1	0.7	−143.6	−2.0
426.827.....	0.591	59.6	−0.9	−126.4	3.6
427.806.....	0.640	45.7	1.2	−105.2	5.8
427.856.....	0.642	44.6	1.1	−104.9	4.9
428.778.....	0.688	21.9	0.1	−84.3	1.5
428.816.....	0.690	19.8	−0.9	−84.3	0.4
429.792.....	0.738	9.0	17.8	−49.3	4.9
429.813.....	0.739	−5.6	3.9	−62.4	−8.9
464.737.....	0.461	71.1	2.5	−144.6	−1.0
465.774.....	0.512	62.7	−8.9	−154.4	−9.0
465.788.....	0.512	71.1	−0.5	−146.2	−0.9
466.756.....	0.560	64.7	−2.4	−139.6	−1.0
467.822.....	0.613	51.1	−3.2	−122.4	0.0
467.836.....	0.613	53.3	−0.7	−119.1	3.1
468.773.....	0.660	35.9	0.0	−95.5	5.8
469.799.....	0.710	0.5	−8.3	−80.7	−8.5
469.813.....	0.711	8.8	0.4	−72.3	−0.6
491.730[b]	0.792	−57.9	−10.0	−9.1	7.4
492.693.....	0.839	−94.4	−9.2	16.9	−0.2
493.677.....	0.888	−125.2	−3.6	46.8	−1.7
494.689.....	0.937	−150.1	0.9	73.2	−0.2
495.747.....	0.990	−162.7	3.5	91.1	4.1
496.742.....	0.039	−161.3	1.0	87.4	1.8
497.700.....	0.086	−144.0	−1.2	68.4	−2.2
516.645.....	0.020	−162.3	3.5	89.6	1.8
517.641.....	0.069	−153.8	−2.6	74.8	−2.6
520.601.....	0.215	−53.9	−4.4	−19.6	−4.1
522.644.....	0.316	16.5	−1.8	−88.2	−0.1

[a]Secondary Phase = Primary Phase – 0.051

[b]Primary – secondary swapped velocities are given and assigned zero weight.

Table 2. Orbital Elements for HD 1383

Element	Hill & Fisher (1986)	This Work
P (days)	20.2819[a]	20.28184[a]
T_1 (HJD–2,400,000)	···	51414.8 ± 0.4
T_2 (HJD–2,400,000)	···	51415.9 ± 0.6
e_1	0.076 ± 0.024	0.116 ± 0.012
e_2	0.027 ± 0.028	0.069 ± 0.009
ω_1 (deg)	181 ± 10	178 ± 6
ω_2 (deg)	355 ± 29	17 ± 10
K_1 (km s^{-1})	113 ± 1	119 ± 1
K_2 (km s^{-1})	117 ± 2	117 ± 1
γ_1 (km s^{-1})	-35.1 ± 1.8	-33.8 ± 1.0
γ_2 (km s^{-1})	-34.7 ± 2.1	-36.5 ± 0.8
q (M_2/M_1)	0.968 ± 0.018	1.02 ± 0.01
$M_1 \sin^3 i$ ($M_\odot$)	12.7 ± 0.2	13.7 ± 0.2
$M_2 \sin^3 i$ ($M_\odot$)	12.4 ± 0.2	13.7 ± 0.2
$a \sin i$ ($R_\odot$)	92.2 ± 0.8	94.2 ± 0.6
σ_1 (km s^{-1})	8.0	5.1
σ_2 (km s^{-1})	9.6	4.3

[a]Fixed.

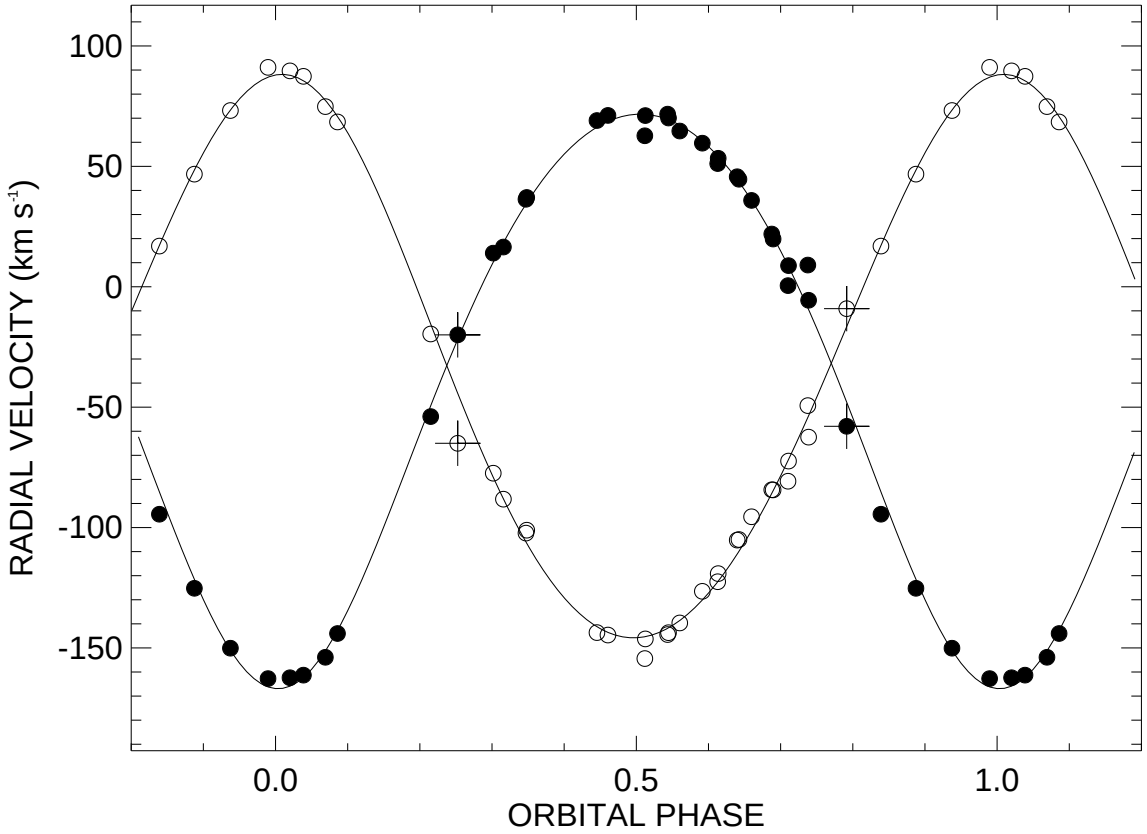

Fig. 1.— Calculated radial velocity curves (*solid lines*) for HD 1383. The errors in the measured radial velocities of the primary star (*filled circles*) and the secondary star (*open circles*) are comparable to the symbol sizes. Plus signs mark the measurements from two blended phases that were assigned zero weight.

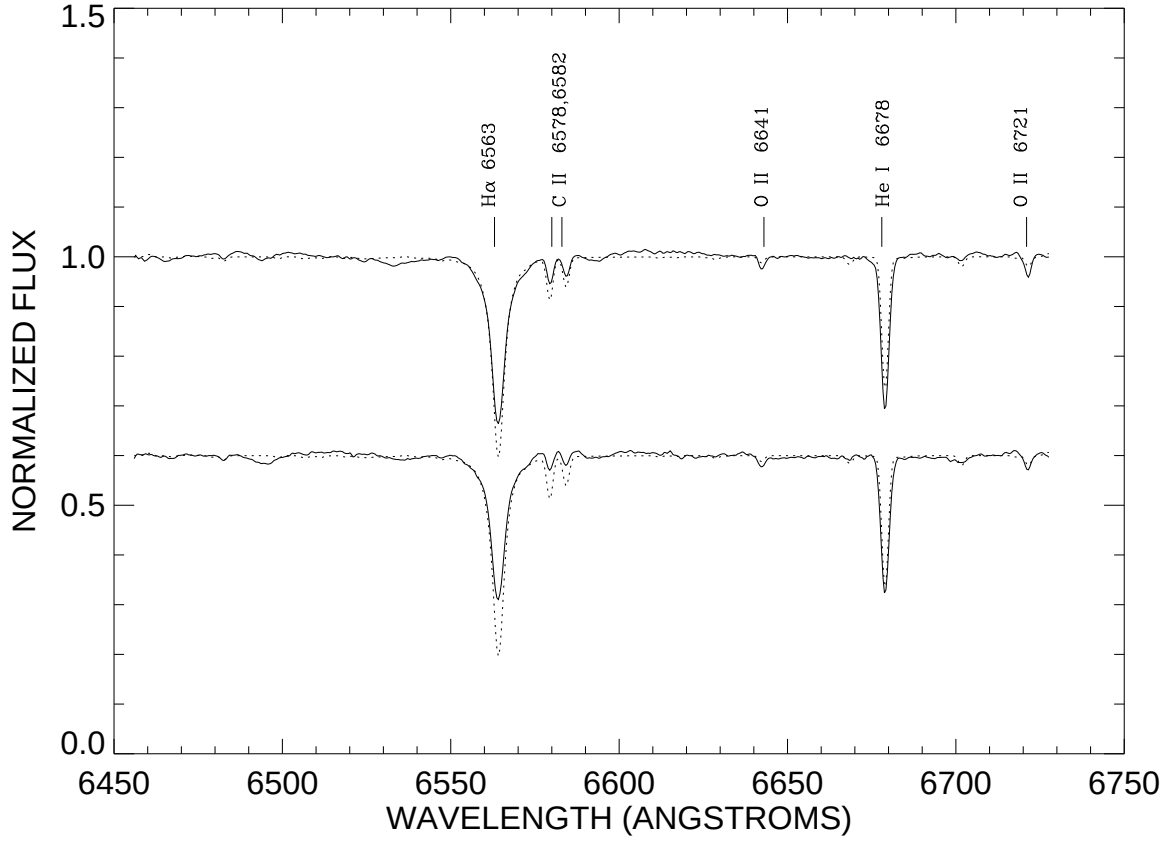

Fig. 2.— The tomographically reconstructed spectra (*solid lines*) of the (slightly more massive) secondary (*top*) and primary star (*bottom*) together with model spectra (*dotted lines*) for $T_{\rm eff} = 28000$ K, $\log g = 3.25$, and $V \sin i = 70$ km s^{-1} (a rotational broadening appropriate for He I λ6678).

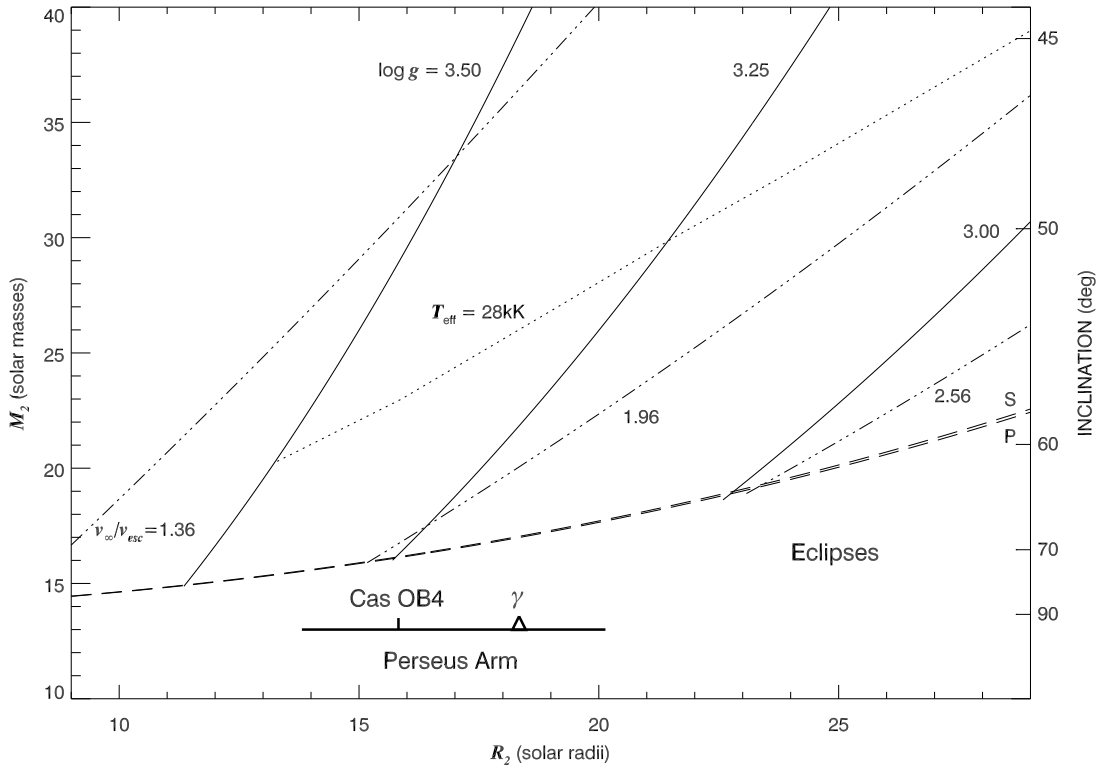

Fig. 3.— A plot of the possible range in secondary mass and radius. The system inclination for $M_2 \sin^3 i$=13.7 is given on the right axis. The dashed lines mark the lower mass limit set by the absence of eclipses and based upon the parameters from the primary (P) and secondary (S) orbital solutions. The three solid lines show the relations for the range in gravity set by the Hα line wings (indicated by values of $\log g$). The three triple dot-dashed lines show the relations set by the span of values for the $v_\infty/v_{\rm esc}$ ratio (with the constant of proportionality labeled in each case). The dotted line indicates the single star evolutionary mass for a temperature of $T_{\rm eff}$ = 28000 K (Schaller et al. 1992). The bar at the bottom shows the corresponding radii for distances spanning a cut through the Perseus arm, the location of the Cas OB4 association, and the location where differential Galactic rotation matches the binary systemic velocity (γ).

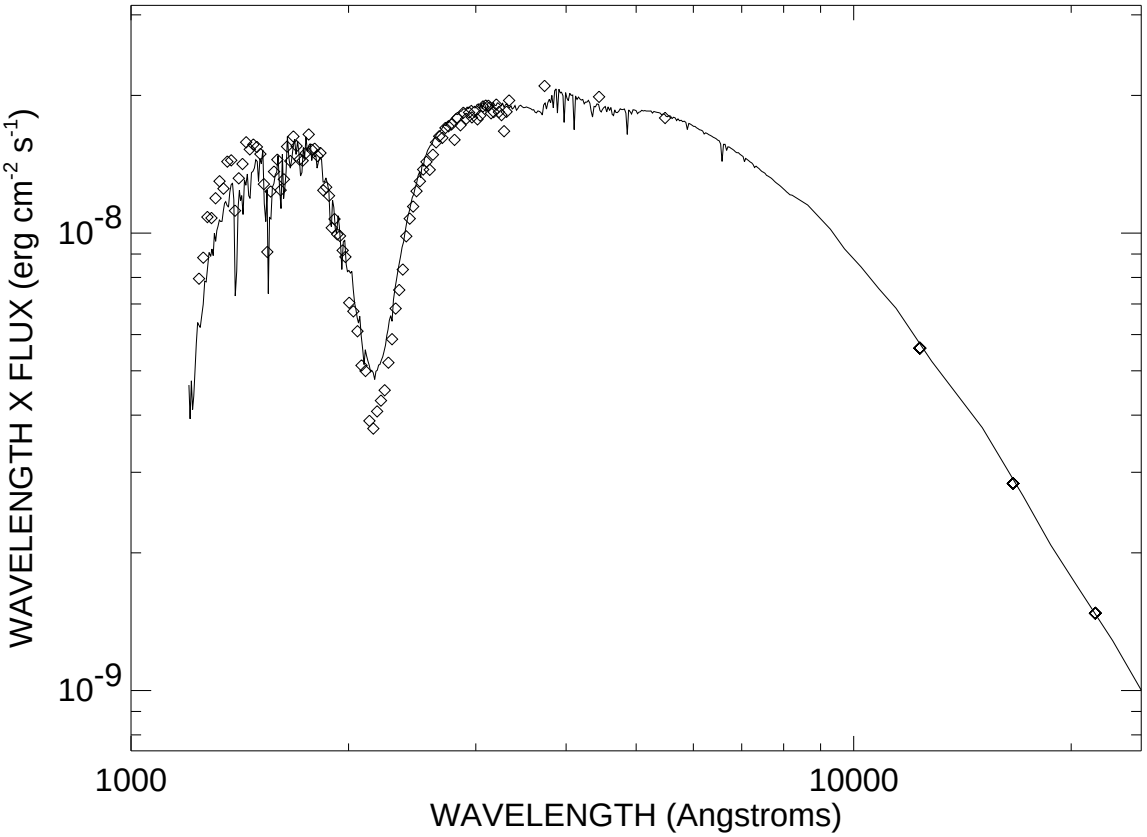

Fig. 4.— The spectral flux distribution and fit for the combined light of the HD 1383 components. The fitting parameters are $T_{\rm eff} = 28000$ K, $\log g = 3.25$, $E(B-V) = 0.55$ mag, $R = 2.97$, and $\theta_{LD} = 54$ microarcsec for each star.

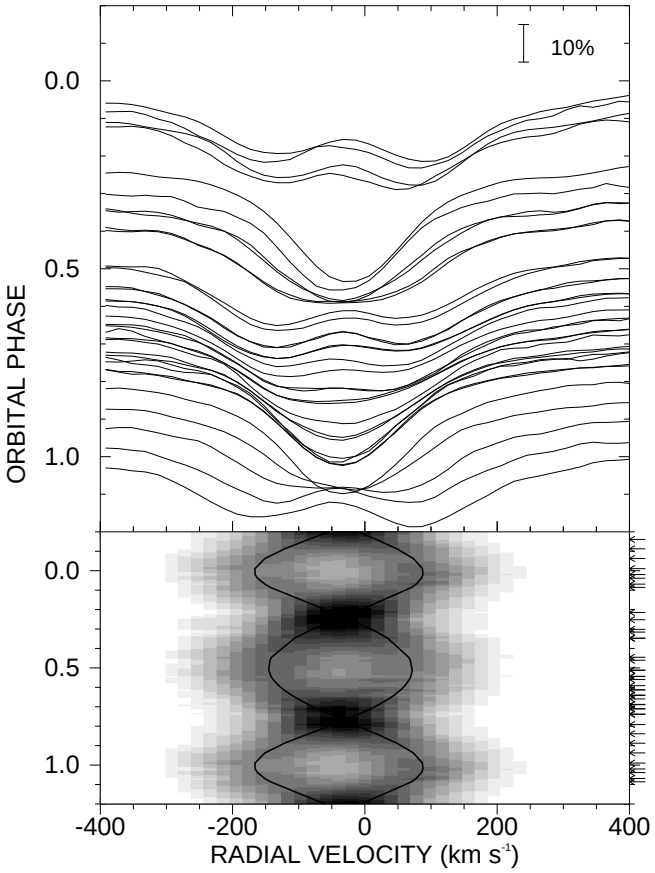

Fig. 5.— *Top:* Hα line profiles plotted against heliocentric radial velocity. The continuum of each observation is normalized so that the y-ordinate equals the primary star phase at the time of observation. *Bottom:* A gray scale plot that shows the phase and velocity variations of the Hα line profiles shown above. Specific times of individual measurements are indicated by arrows on the right hand side. There are 16 gray levels that are determined by the difference in intensities between the minimum to maximum observed values for all spectra. The phase has been wrapped to enhance the sense of phase continuity, and the calculated radial velocity curves from the orbital solution are displayed as thick black lines.